*Physics – Uspekhi* **67** (2) 157 – 170 (2024) 

*REVIEWS OF TOPICAL PROBLEMS*

PACS numbers: **42.65. – k,** 52.38.Hb, 52.59.Ye

*40th ANNIVERSARY OF THE PROKHOROV GENERAL PHYSICS INSTITUTE, RUSSIAN ACADEMY OF SCIENCES*

# Generation of terahertz radiation in the plasma of optical gas breakdown

A A Ushakov, P A Chizhov, V V Bukin, S V Garnov

DOI: https://doi.org/10.3367/UFNe.2023.10.039579

## Contents



**Abstract. The paper presents the current state of research on the generation of terahertz radiation in the optical breakdown of gases by laser radiation, consisting of the fundamental and second harmonics of femtosecond laser radiation. We consider the main approaches to describing the generation of terahertz radiation. The influence of the focusing mode, spatial and temporal modulation, changes in the wavelength, and polarization state of the pump radiation is shown. Also considered is the influence of the properties of the medium into which laser radiation is focused.**

**Keywords:** femtosecond laser plasma, filamentation, terahertz radiation

**A A Ushakov** [1, a], **P A Chizhov** [1, 2, 3, b], **V V Bukin** [1], **S V Garnov** [1, c]
[1] Prokhorov General Physics Institute, Russian Academy of Sciences, ul. Vavilova 38, 119991 Moscow, Russian Federation
[2] Moscow Institute of Physics and Technology (National Research University), Institutskii per. 9, 141701 Dolgoprudnyi, Moscow region, Russian Federation
[3] Russian Institute for Scientific and Technical Information (VINITI RAS), ul. Usievicha 20, 125190 Moscow, Russian Federation
E-mail: [a] ushakov.aleksandr@physics.msu.ru, [b] pvch@inbox.ru, [c] garnov@kapella.gpi.ru

Received 11 August 2023, revised 6 October 2023
*Uspekhi Fizicheskikh Nauk* **194** (2) 169 – 183 (2024)
Translated by E N Ragozin

## 1. Introduction

The development of ultrashort pulse lasers has led to the possibility of studying high-order nonlinear effects, such as the generation of higher-order harmonics, filamentation, and optical breakdown. In particular, the optical breakdown of gaseous media with the formation of nonstationary plasma — a source of secondary radiation — has become possible. The role of secondary radiation is played not only by optical (generation of a supercontinuum with components in the blue part of the spectrum [1], lasing [2], high-order harmonics [3], X-ray and $\beta$-radiation [4], etc.) but also by far infrared radiation, which is also called submillimeter or terahertz (THz) [4]. The first paper on the generation of pulsed terahertz radiation during the interaction of ultrashort pulses with matter was published back in the late 1980s [5]: for a source, it used a semiconductor antenna, but even then the broad prospects for using pulsed sources in this range of the electromagnetic spectrum were shown due to the possibility of direct measurement of the temporal shape of THz pulses. For this and other fundamental physical reasons (the presence of isolated rotational and vibrational modes in a number of substances in the THz range, strong absorption in water and weak absorption in plastic, low photon energy, weak scattering, etc. [6, 7]), interest in this range is steadily rising nowadays.

While on the subject of laser plasma as a source of THz radiation, the first papers on this subject were published in 1993–1994 [4]. They demonstrated the generation of pulsed THz radiation with a duration of about 1 ps when femtose-

cond laser radiation with a duration of about 100 fs and an energy of up to 50 mJ was focused into gases and solid-state targets. The main mechanism for generating terahertz radiation in this case is the radial pondermotive action of radiation on ionized electrons in the plasma, which largely explains the rather low optical-to-terahertz conversion efficiency of $\sim 10^{-7}-10^{-9}$, the relatively narrow generation spectrum, and conical emission at an angle to the axis plasma channel. It is noteworthy that, in addition to THz radiation from the plasma, $\beta$-radiation of accelerated electrons from the plasma and hard X-ray radiation were recorded, and also that all three mentioned types of radiation correlated with each other.

To optimize this generation method, axicon focusing was later proposed, whereby an incident laser beam was focused into a filament elongated along its axis. In this case, a superluminal ionization wave appears along the axis with a speed $V = c/\sin\theta$, where $\theta$ is the focusing angle of the lens. In the presence of an external electric field, plasma polarization occurs during ionization. As a result of polarization, a wave of plasma oscillations current travels at superluminal speed, emitting an electromagnetic pulse due to the Cherenkov mechanism [8].

All of the above methods are usually used in facilities with relatively high laser pulse energies (tens of mJ) and relatively low pulse repetition rates (units to tens of Hz). Other methods are necessary to work at facilities with lower energy levels (several mJ per pulse) but, as a result, more available to research laboratories and, in addition, having kHz laser pulse repetition rates. These laser systems already provide the radiation intensity necessary for ionization, but other approaches are required to accelerate electrons in the plasma. The application of an external static electric field to the plasma production region resulting from photoionization provides a relatively strong electron acceleration. This, in turn, increases the photocurrent, which determines the efficiency of terahertz radiation production. The direction of the photocurrent in this case coincides with the direction of the electrostatic field; the application of the field in the direction perpendicular to the direction of propagation of the laser pulse will result in a coherent increase in the strength of the THz radiation pulse along the plasma channel. For microwave radiation, this approach was shown in 1996 [9], and the same idea was transferred for generation in the THz range at the turn of the 2000s [10]. The demonstrated method made it possible to improve the optical-to-terahertz radiation conversion efficiency by an order of magnitude over previously proposed methods of pondermotive acceleration of electrons without an external field. First of all, the radiation intensity generated in the THz range was determined by the magnitude of the applied electrostatic fields, which were limited by the breakdown threshold. More recently, a method was proposed in which the electron acceleration in plasma occurred under the influence of femtosecond laser radiation at the fundamental frequency and the second harmonic [11]. In the first work, the generation scheme was based on placing a second harmonic crystal in a converging laser beam after the focusing lens. The main interpretation of the resulting generation was initially considered to be optical rectification during four-wave mixing (the case of generation of a difference frequency close to a quasi-constant field). Subsequently, for a number of reasons, this model was revised and supplemented. A remarkable distinctive property of this generation method, which sets it apart from others, is the ultra-broad 0.1–200-THz spectrum of generation of THz radiation, the ability to focus laser radiation directly in front of the object under study to produce a source, which will avoid natural loss in the THz beam associated with absorption by water vapor during radiation propagation in the atmosphere. In general, there are studies that combine the two above approaches to the generation of terahertz radiation in plasma (two-color pumping + external field) [12, 13] in order to increase the generation efficiency and control the terahertz radiation parameters.

It is pertinent to note that there are other media apart from gases, in which the formation of plasma under the influence of ultrashort laser radiation leads to the generation of THz pulses. One of the interesting experiments in this regard is the generation of THz radiation during the interaction of femtosecond laser pulses with a gas jet, which produces clusters in the expansion into a vacuum for a certain nozzle shape [14]. Also observed in this case is the generation of X-ray radiation together with terahertz radiation. A distinctive property of the clusters themselves is the high absorption coefficients for laser radiation at a relatively low particle density [15]. Also noteworthy is the fact that the optical-to-terahertz conversion efficiency in this case is significantly higher in the presence of a prepulse, which preheats the medium into which the main pulse is sent, producing a plasma channel [16].

By analogy with gas jets, the generation of THz radiation by irradiating droplets of liquid metal with femtosecond laser radiation was demonstrated [17]. For a relatively low optical-to-terahertz conversion efficiency ($\sim 10^{-8}$), an increase in the output energy of THz radiation is also observed with the use of two pulses: one that heats the medium and a high-power one that directly gives rise to the generation.

Despite the seeming impossibility of effectively generating THz radiation in liquids due to their strong absorption, similar studies have been carried out by different groups. Moreover, relatively efficient emission was demonstrated both in a thin film of liquid [18–20] and in an extended cell [21]. An interesting fact is that, in the case of a thin film, the presence of a heating prepulse also leads to an increase in the output power of the generated THz pulse [19].

So, to date, the generation of terahertz radiation using femtosecond laser radiation has been demonstrated in various media and it is absolutely impossible to fit all current trends on this issue into one review paper. An attempt to include all the results will lead to the need to limit the listing of numerous results, while it will be more useful to examine a number of key issues in more detail than to superficially familiarize ourselves with the entire variety of papers. Therefore, we will dwell thoroughly on a detailed discussion of the issues of generation of terahertz radiation when focusing femtosecond laser radiation into gaseous media at the fundamental and second harmonics in view of the ultra-broad spectrum of generation of secondary radiation (see Table 1) and the prospects for using these sources in remote diagnostics and spectroscopy.

This review presents the current state of research on the generation of terahertz radiation in the optical breakdown of gases by laser radiation consisting of the fundamental and second harmonics of femtosecond laser radiation (hereinafter this radiation will be referred to as two-frequency or two-color, and the optical breakdown plasma produced by such radiation will be referred as two-color plasma). Section 2 presents general approaches to describing the generation of terahertz radiation in gaseous media. Section 3 presents research aimed at optimizing the polarization state of the

**Table 1.** Methods for generating high-intensity THz radiation.

| Method | Electric THz field strength, MV cm$^{-1}$ | Photon energy conversion efficiency | Central spectrum frequency, THz | Spectral emission band, THz |
|---|---|---|---|---|
| Two-color laser plasma (0.8 + 0.4 μm) [22] | 8 | $10^{-4}$ | ~ 2 | > 100 |
| Two-color laser plasma (3.9 + 1.95 μm) [23] | 100 | $2.4 \times 10^{-2}$ | ~ 8 | ~ 15 |
| Gas cluster plasma [24] | — | $10^{-7}$ | ~ 0.4 | ~ 1 |
| Optical rectification [25] | 83 | $3 \times 10^{-2}$ | ~ 4 | ~ 5 |
| Optical rectification with inclined front in $LiNbO_3$ [26] | 7.5 | $10^{-2}$ | ~ 0.3 | ~ 1.3 |
| Photoconductive antenna [27] | < 1 | $10^{-6}$ | ~ 2 | ~ 5 |
| Plasma in thin layers of liquid [18, 19, 28] | 0.2 | ~ $10^{-4}$ | ~ 1–1.5 | ~ 2–3 |
| Emission by a short electron bunch [29] | 200 | $10^{-4}$ | — | > 10 |
| Free-electron laser [27] | 2 | $10^{-3}$ | 3 | ~ 10 |

waves of a two-frequency pump, with emphasis placed on the case when pulses at the fundamental and second harmonics are formed in different optical arms. Section 4 considers the issue of the most optimal mode for focusing two-frequency laser pulses for generating THz radiation in the plasma produced and considers both the issue of energy parameters and the directional pattern of the output radiation. The case of sharp focusing with the formation of THz radiation propagating towards the pump pulses is especially highlighted, and the features of this radiation are considered. The features of the generation of terahertz radiation in extended plasma channels are also considered, when interference effects are observed in the resulting terahertz pulse, which can be used to control the carrier-envelope phase and frequency filtering of the radiation. Section 5 examines the effect of modulation of laser pulses on the generation of THz radiation in plasma. Section 6 is devoted to determining the influence of the pump radiation wavelength. Section 7 is concerned with the influence of the properties of gaseous media (pressure, chemical composition) on the generation of terahertz radiation. Section 8 discusses the issue of superfilamentation, an especially relevant mode of interaction of laser radiation with gases nowadays.

## 2. Generation of terahertz radiation in the focusing of two-color radiation into gaseous media. Description of generation mechanisms

To describe the mechanism of generating terahertz radiation by focusing two-color femtosecond laser radiation into gaseous media, it was initially proposed to use the formalism of third-order nonlinear polarization [11], namely the generation of a difference frequency, which can be formally described as $\omega + \omega' - 2\omega = \Omega_{\mathrm{THz}}$. This approach successfully describes a number of experimental curves, for example, the power-law dependence of terahertz radiation energy on the energy of laser radiation [11, 30, 31]. In addition, noteworthy is the sinusoidal dependence of the THz radiation power on the position of the second harmonic crystal along the optical axis [30], which is explained by a shift in the relative phase difference between the first and second harmonics due to dispersion. However, there are a number of inconsistencies with the proposed model, for example, the presence of saturation with increasing laser radiation intensity [32] and an anomalously high value of nonlinear susceptibility [30]. It is noteworthy that the presence of a prepulse, which ionizes the gas before the arrival of the main high-power pulse, significantly reduces the efficiency of terahertz radiation production [33, 34]. A number of these facts led to another description method associated with field ionization of gaseous media by femtosecond laser radiation and the production of nonstationary photocurrents [34]. Field ionization, which is quite successfully described by formulas [35–37], gives rise to free electrons accelerated by laser pulses. The presence of a nonzero phase difference between the first and second harmonics leads to a violation of the symmetry of the field acting on the electrons, which in turn allows the production of a nonzero photocurrent, the derivative of which is proportional to the terahertz field strength. This model also successfully describes the sinusoidal curve of THz radiation energy at the position of the second harmonic crystal along the axis [34], since the relative phase between the first and second harmonics significantly affects the formation of a nonzero photocurrent that determines the terahertz field.

More clearly, the formation of a source of THz pulses in the focusing of two-color laser pulses into gaseous media can be considered as follows. At the first stage, during which there is no direct ionization of the medium yet, a high-intensity laser field entails a nonlinear response of neutral atoms and molecules. This response can be considered within the framework of the third-order nonlinear susceptibility mechanism, which is described using the Fourier transform operator $\hat{F}$ by the formula [38]

$$\hat{F}(\ddot{\mathbf{P}}) = -\omega^2 \chi^{(3)}_{1111} \hat{F}(|\mathbf{E}|^2 \mathbf{E}), \; S_{\mathrm{pol}}(\omega) = |\hat{F}(\ddot{\mathbf{P}})|^2 . \tag{1}$$

Here, $\ddot{\mathbf{P}}$ is the second time derivative of polarization, $S_{\mathrm{pol}}$ is the spectral intensity, $\omega$ is the circular frequency of the radiation, $\mathbf{E}$ is the field strength, and $\chi^{(3)}_{1111}$ is the third-order nonlinear susceptibility tensor.

At the second stage, direct field ionization of the gaseous medium occurs. In this case, the generation of THz radiation is described in the framework of the nonstationary photocurrents model using the following equation [38]:

$$\hat{F}(\dot{\mathbf{J}}) = \frac{\omega}{\omega + \mathrm{i}\nu_{\mathrm{c}}} \left( \frac{e^2}{m} \hat{F}(\mathbf{E} N_{\mathrm{e}}) + e\hat{F}\left(\mathbf{V}_{\mathrm{e}}(t,t)\dot{N}_{\mathrm{e}}\right) \right),$$
$$S_{\mathrm{pc}}(\omega) = |\hat{F}(\dot{\mathbf{J}})|^2 , \tag{2}$$

where $N_e(t)$ is the total electron density at point in time $t$, $\mathbf{V}_e(t,t)$ is the initial velocity of electrons produced at point in time $t$, $e$ and $m$ are the electron charge and mass, $\nu_c$ is the collision frequency, $S_{pc}(\omega)$ is the spectral intensity of photocurrent, and $\dot{\mathbf{J}}$ is the photocurrent time derivative.

Considered at the third stage is the generation of THz radiation in an already formed plasma. Here, the mechanism of third-order nonlinear plasma susceptibility is used for the description. Using the method of successive approximations, the corresponding formula was obtained for determining the contribution of the Lorentz force $G_x$, which determines the generation of THz radiation [39]:

$$G_x = -\frac{e^3}{8m^2c^3(\gamma^2+\omega^2)(\gamma^2+4\omega^2)}\left[E_\omega^2 E_{2\omega}^* + \text{c.c.}\right]. \quad (3)$$

In this formula, $\gamma$ is the collision frequency, and $E_\omega$ and $E_{2\omega}^*$ are the fields of the fundamental and second (complex conjugate) harmonics.

More recently, the contributions from these two proposed models — third-order nonlinear polarization and nonstationary photocurrents — were compared in Refs [38, 40]. It was shown that the dominant contribution to the formation of terahertz pulses occurred due to the production of photocurrents, while the spectrum of electromagnetic emission from plasma in the low-frequency region is dominated by the signal from nonstationary photocurrents, and in the high-frequency region, by third-order nonlinear polarization.

Subsequently, these two approaches were combined within a single model, described by the so-called unidirectional pulse propagation equation (UPPE) [40–42]. This equation is often written for the axially symmetric spatiotemporal Fourier harmonic

$$\left(\frac{\partial}{\partial z} + ik_z\right)\hat{E}(\omega,k_r,z) = -\frac{2\pi\omega}{c^2k_z}\left(\hat{J}(\omega,k_r,z) + i\omega\hat{P}(\omega,k_r,z)\right), \quad (4)$$

where $z$ is the propagation coordinate and $c$ is the speed of light. This propagation equation is most suitable for modeling the generation of THz radiation from plasmas induced by two-frequency femtosecond pulses, since it describes both the electric field with an ultra-broad spectrum, from THz to ultraviolet, and nonparaxial diffraction (this is especially important for low-frequency THz components of the spectrum, which can diverge from the filament at angles of $\sim 10^\circ$ or more) in terms of the longitudinal wave number $k_z(\omega,k_r) = [\omega n^2(\omega)c^{-2} - k_r^2]^{1/2}$, where $n(\omega)$ is the refractive index. The equation for unidirectional propagation of radiation includes the response to third-order nonlinear polarization (Kerr effect) $\hat{P}$ [11, 43] and nonstationary photocurrent $\hat{J}$ [31, 43]

$$\left(\frac{\partial}{\partial t} + \nu_c\right)J(t,r,z) = \frac{e^2}{m_e}N_e(t,r,z)E(t,r,z). \quad (5)$$

Here, $m_e$ and $e$ are the electron mass and charge, and $N_e$ is the free electron density described using the equation

$$\partial_t N_e = w\left(E(t,r,z)\right)\left(N_0 - N_e(t,r,z)\right), \quad (6)$$

where $w(E)$ is the ionization probability [35]. In general, this approach is currently one of the most common and widely used in practice for interpreting and describing experimental data.

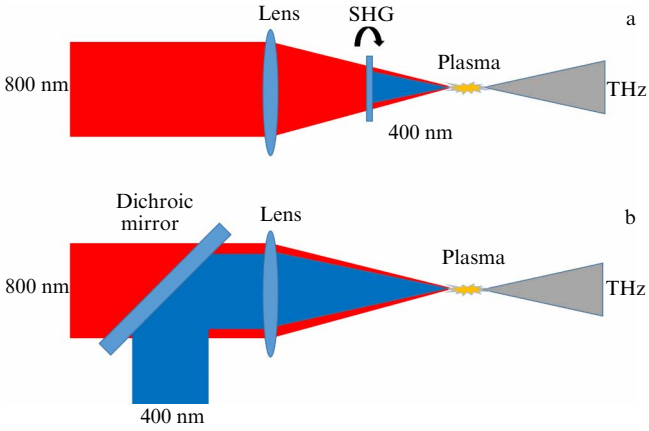


**Figure 1.** Mechanisms for generating terahertz radiation in laser plasma: (a) pump polarization is controlled by rotating the converter crystal (second harmonic generator); (b) pump polarization is controlled independently; two-color pulse is formed after the dichroic mirror.

## 3. Investigation of the effect of the polarization state of two-frequency pump radiation

In pioneering study [11], the polarizations of the components of a two-color pulse were linear orthogonal, since a type-I phase matching crystal was used to obtain the second harmonic. Assuming that terahertz radiation is produced in four-wave mixing, the co-directional state of harmonic polarizations should provide a better result. Further studies were aimed at determining the components of the nonlinear susceptibility tensor $\chi^{(3)}$ and determining the dependence of terahertz radiation polarization on the state of polarizations of the two-color pump components. In Ref. [30], a rotation of the type-I phase-matching crystal relative to the optical axis was used (Fig. 1a). In doing this, the angle between the polarization directions of the fundamental and second harmonics changed, but at the same time the radiation conversion efficiency to the second harmonic also changed. For a fixed conversion efficiency to the second harmonic and relative rotation of the linear polarizations of the harmonics, the generation efficiency of p-polarized terahertz radiation was studied in Ref. [44] to determine the components of the $\chi^{(3)}$ tensor. In this work, the radiation was divided into two beams (Fig. 1b) and mixed together with a dichroic mirror. It is worth noting that, in this configuration, the phase between the harmonics experiences beats due to various inhomogeneities along the path of the beams, and restoring the temporal shape of the terahertz pulse is a nontrivial task. In Ref. [45], both polarizations (s- and p-polarized) were recorded in setups similar to those mentioned [30, 44]. A more thorough analysis of pump polarizations was carried out and the cross components of the nonlinear susceptibility tensor were identified.

With the advent of the transient photocurrent model [34], there is a departure from determining the components of the nonlinear susceptibility tensor to considering the photoionization and trajectories of electrons that should emit terahertz radiation. It is worth noting that the proposed model also contains a harmonic dependence on the relative phase between the components of the two-color pulse. However, the efficiency of terahertz radiation production is related to the ionization rate, which nonlinearly depends on the total instantaneous intensity of the two-color field. Mention

should be made of Ref. [46], where the polarization state of terahertz radiation varies widely due to the use of circular polarization of the fundamental harmonic, while the second harmonic is polarized weakly elliptically (in generation in a type-I matching crystal) with a 1 to 11 aspect ratio of the polarization ellipse axes. It is also worth noting Refs [47–49], whose authors demonstrated the feasibility of stabilizing the average power of THz emission through the use of elliptical harmonics polarizations when using a generation scheme with an unstable phase between harmonics (Fig. 1b).

J-M Manceau et al. [50] noted the effect of polarization variation (rotation) of the terahertz radiation generated by two-color pulses depending on gas pressure. The authors attribute it to a pressure-dependent phase change between harmonics due to dispersion in the gas, as well as to the presence of birefringence in plasma for a terahertz pulse, which may result in ellipticity of the THz radiation polarization up to circular.

In Ref. [51], the polarization state of terahertz radiation was experimentally studied in relation to the relative rotation angle of linearly polarized harmonics and analyzed using numerical simulation using a unidirectional pulse propagation equation with the inclusion of free (photocurrents) and bound (nonlinear susceptibility) charge carriers. It was shown that the polarization of terahertz radiation is mainly close to linear and co-directed with the polarization of the fundamental harmonic; however, near the rotation angle of the harmonic polarizations, in the range of $60^\circ - 90^\circ$, a transition occurs to elliptical polarization with a maximum ellipticity of about $85^\circ$. And then, with orthogonal polarizations of the harmonics, the terahertz polarization becomes linear and co-directional with the polarization of the second harmonic.

Among recent publications, mention should be made of Ref. [52], where co-directional circular polarizations of harmonics are used for generation, which leads to an eight-fold increase in conversion efficiency compared to the case of co-directional linear harmonic polarizations. It should also be noted that the peak frequency in the spectrum of terahertz radiation shifts when use is made of elliptically polarized harmonics [53].

The chirp of the laser pulse also has a significant effect on the polarization of the emitted terahertz pulse in the case of using elliptical polarization of the fundamental harmonic and weakly elliptical polarization of the second one (when generated in a rotated crystal of type-I phase matching). The effect is associated with a mismatch in the relative phase between harmonics; when the sign of the chirp changes, a reversal is observed in the rotation direction of THz radiation polarization [54].

## 4. Effect of laser radiation focusing mode

It is a well-known fact that focusing two-color radiation with a lens, where the generation of the second harmonic occurs before the radiation passes through the lens, inevitably entails chromatic aberrations on the one hand and dispersion effects on the other. This means that the harmonics have different effective focal lengths and diverge in time and space, thereby reducing the generation efficiency. However, in Ref. [55], a method was proposed for independently focusing the first and second harmonics into a gaseous medium. In this case, by adjusting the position of the lens in one of the arms, it is possible to achieve coincidence of the focal positions for both harmonics, and by changing the delay between the harmonics, it is possible to realize their overlap in time, thereby improving the efficiency of THz generation. In general, this problem is solved by using parabolic mirrors to focus two-color pumping due to the absence of dispersion and chromatic aberrations.

### 4.1 Investigation of the directional terahertz radiation pattern in relation to the focusing mode

One of the key areas in the study of laser-plasma THz radiation sources is the determination of the radiation pattern of the output radiation. In the first paper [56], the directional pattern of THz radiation from a plasma produced by different focusing of two-color laser radiation was studied using a slit aperture and a balanced detector. A transition from a unimodal (with an on-axis maximum) to a ring structure was demonstrated when the pump radiation focusing mode was changed. More recently, this issue was studied in other publications; a high angular divergence and conical structure of THz radiation from a filament [56–65] have been demonstrated, which generally reduce the potential applicability of these sources. Therefore, there is a need to optimize the conditions for generating THz radiation in a dual-frequency configuration.

Simultaneously with the generation of terahertz radiation, transformation of optical harmonics occurs in a two-frequency filament in the air [51, 66]. This effect is due to both the instantaneous nonlinear electronic response [43] and the inertial molecular response [67].

The total divergence of THz radiation is determined primarily by the length of the plasma channel $L_{\text{fil}}$, and the divergence angle $\theta$ is approximately proportional to the value $(\nu_{\text{THz}} L_{\text{fil}})^{1/2}$, where $\nu_{\text{THz}}$ is the THz radiation frequency [57, 59, 62, 68, 69]. The conical structure in the case of a dual-frequency filament arises due to a phase mismatch [59] and plasma-induced scattering [62, 64]. The phase mismatch effect provides an off-axis phase match for THz radiation due to the inversion of its polarity with an increase in the phase shift between optical harmonics from 0 to $\pi$. This mechanism is important for plasma channels with a length of 2 cm or more. The plasma forces out the THz radiation due to a strong refractive index gradient inside and outside the channel. The experiments and simulations of Refs [61, 64] suggest that a bright ring-shaped structure in the angular distribution is produced in the high-frequency region $\geqslant 3$ THz, while the distribution at lower THz radiation frequencies ($\sim 1$ THz) remains more unimodal [58, 61, 64]. This means that the transition from a unimodal structure to the annular one occurs in the frequency region of about 0.3–3 THz. In early studies, the angular distribution in the spectral range up to 3 THz was measured quite coarsely, although frequency-angular distribution measurements [61, 64] were performed in the range up to 10–15 THz. Later, more detailed investigations of frequency-angular distributions in the low-frequency region of the terahertz range were carried out. In Ref. [42], comparative measurements of frequency-angular distributions were performed using two methods: (i) a Golay detector with a narrow-band THz filter on the input window was located at different angles to the optical axis; (ii) an electro-optical balanced detector was located at different angles to the axis, which measured the temporal shape of THz radiation pulses, and then the spectrum was reconstructed using the Fourier transform. The studies were carried out on laser systems with pulse durations of 35 and 150 fs. The frequency-angular distributions are illustrated in Fig. 2.

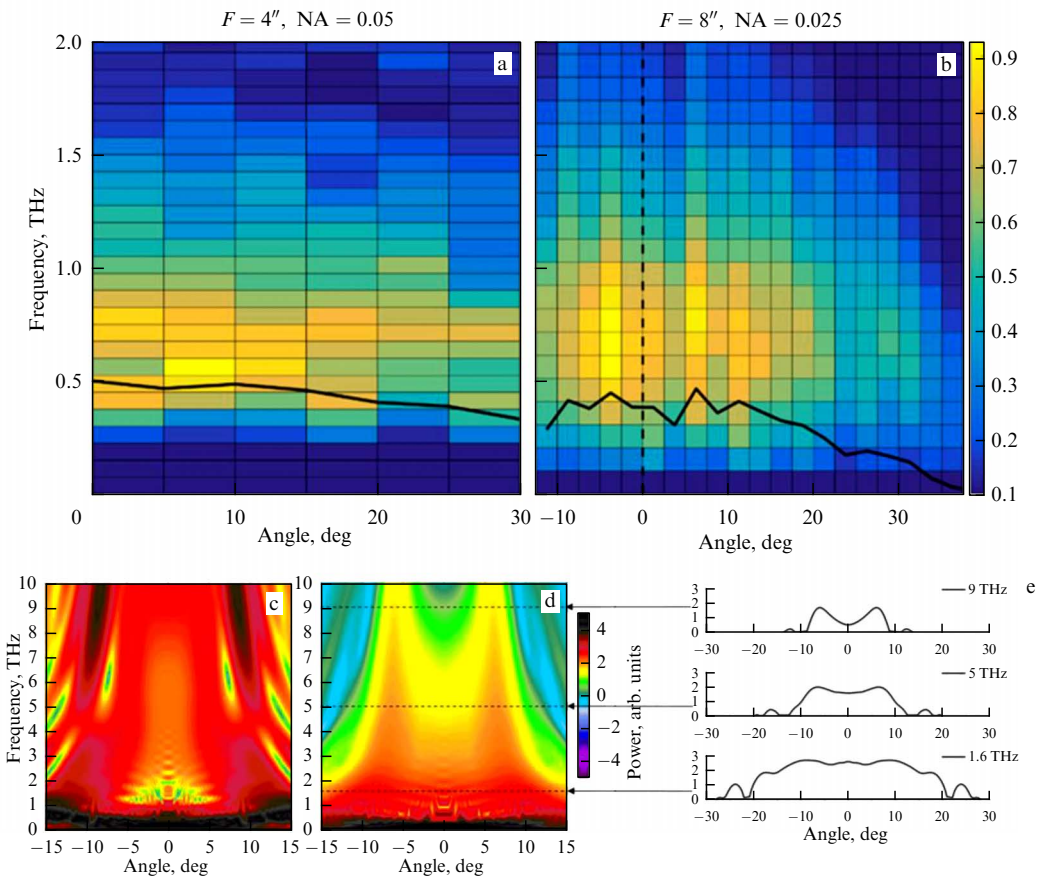


**Figure 2.** Frequency-angular distributions of THz radiation power measured for various numerical apertures (NAs) of parabolic mirrors (a, b) and obtained as a result of numerical simulation within the framework of the unidirectional radiation propagation equation (NA ≈ 0.05) (c), (NA ≈ 0.025) (d), with angular distributions for certain frequencies on a linear scale (e).

Within the framework of measurements and simulations, the range of numerical apertures (NAs) $\approx 0.2-0.02$ was considered. The angular diagrams of THz radiation were shown to be similar for both laser systems. This testifies that the divergence of THz radiation in the low-frequency range is determined mainly by the focusing conditions of the laser pump radiation, while the dependence on the pulse duration is much weaker. For sharper focusing, the THz emission distribution is unimodal; the sharper the focusing, the broader the output radiation pattern. On the contrary, the distribution of THz radiation for softer focusing (NA $\approx 0.025-0.02$) was narrower (divergence angles of $15^\circ-40^\circ$ to the optical axis), with a pronounced annular structure with a divergence angle to the axis of $7^\circ$.

The results obtained in experiments and numerical simulations were explained on the basis of two mechanisms: phase mismatch between optical harmonics, leading to a change in the polarity of THz pulses [59], and scattering by dense plasma as an obstacle to THz radiation [62, 64]. But given that the length of the plasma channel did not exceed 7 mm and the length of the mismatch between the harmonics was about 2 cm, it was concluded that the appearance of the annular structure was mainly determined by THz radiation scattering by the plasma as an obstacle. With a plasma channel diameter of about 100 μm, it is a subwavelength obstacle to THz radiation with a frequency $\nu_{\mathrm{THz}} \leqslant 3$ THz (wavelengths greater than $\approx 100$ μm). Low-frequency THz waves bend around such an obstacle without significant changes in the far-field diffraction zone, even when the plasma frequency is higher than the THz radiation frequency. As a result, low-frequency THz radiation is unimodal without annular structures.

By contrast, THz waves with a frequency $\nu_{\mathrm{THz}} \geqslant 3$ THz (wavelengths shorter than $\approx 100$ μm) diffract less efficiently in the plasma channel and, therefore, propagate through the plasma [42]. This results in a plasma-induced phase shift between harmonics, which leads to an annular distribution of THz radiation power in the far-field diffraction zone. A longer plasma channel enhances this effect and can be observed for lower frequency THz waves.

By and large, plasma-based sources have a conical structure in frequency-angular distributions; with an increase in the numerical aperture, the ring structure shifts to the high-frequency region, but at the same time the THz pulse energy decreases. In this case, a question arises about the most optimal use of such sources for materials research tasks, for example, using the *Z*-scan technique. As shown in Ref. [70], even for a strongly pronounced annular structure of THz emission, there is a region of uniform unimodal distribution near the waist of the parabolic mirror which collects the radiation from the source. Therefore, the lack of plasma-based sources in the form of an annular emission pattern can be compensated for by optimizing experimental conditions.

### 4.2 Generation of terahertz radiation in plasma in the direction opposite to the propagation of pump radiation

Sharp focusing of laser radiation leads to the production of a microplasma source, whose spatial scale is of the same order of magnitude as the wavelength of the generated radiation. As a

result, such sources generate THz radiation at angles close to 90° relative to the optical axis [63, 65]. In general, the possibility of observing terahertz radiation in the direction opposite to the propagation of laser radiation was theoretically predicted (hereinafter, this radiation will be referred to as backward, and the THz radiation copropagating with the pump radiation, as forward) thanks to the interference model [69, 71] (the plasma channel is assumed to be a set of sources whose wave interference makes up the directional radiation pattern) and using a numerical solution of the Schrödinger equation together with the interference model [72]. Backward terahertz emission was experimentally observed for the first time only for an argon jet with clusters irradiated by single-color laser radiation [24]. For two-color pumping, backward terahertz radiation from a laser plasma was recorded in Ref. [73]. To record the backward THz radiation, a quartz plate coated with a thin layer of indium tin oxide (ITO), which transmitted optical radiation and reflected terahertz radiation, was inserted at an angle into the optical beam before a parabolic mirror intended for focusing the laser radiation. The parabolic mirror simultaneously served as a collimator for backward THz radiation, since the source, the microplasma, was at the focus. After the ITO-coated quartz plate, the radiation was focused into a Golay detector, and the THz radiation power in the forward direction was also independently recorded. The comparative ratio of the terahertz radiation power in the forward and backward directions gave a value of 5%, which was in good agreement with the simulation data taking into account the real apertures of the optical elements used for the experiments. More recently, a more detailed analysis of the properties of backward terahertz radiation was performed in Ref. [74]. For example, it was shown that the backward-to-forward direction power ratio decreases with the length of the plasma channel. Analysis of the temporal pulse shapes obtained using standard time-resolved electro-optical detection techniques [75, 76] showed that the spectrum of backward radiation has a low-frequency shift compared to the spectrum of forward THz radiation. To verify the results, corresponding numerical modeling was carried out within the framework of the interference model, which made it possible to calculate the transfer function $\epsilon$, defined as the backward-to-forward radiation power ratio for different frequency components. These dependences are presented in Fig. 3. Comparative analysis confirms the spectral shift of 0.1 to 1 THz to the low-frequency side for backward THz radiation compared to the spectrum of forward THz radiation; this is caused by the convergence of the plasma channel to a point source with decreasing frequency.

Later study [77] also confirms the above observations about the low-frequency shift of the backward radiation spectrum and the dependence of the energy ratio on the channel length. A remarkable fact is the channel-length-dependent shift in the arrival time of the backward THz radiation pulse at the detector, which is related to the pump radiation power. Increasing the power leads to a shift in the focus position due to the self-focusing effect, thereby changing the source position versus laser radiation energy.

Spectral measurements of backward THz radiation make it possible to estimate the spectrum of THz radiation in the forward direction and the length of the plasma channel by measuring the parameters of backward THz radiation. So, all these results can be useful for noninvasive diagnostics of the parameters of forward/backward THz pulses using the parameters of the other.

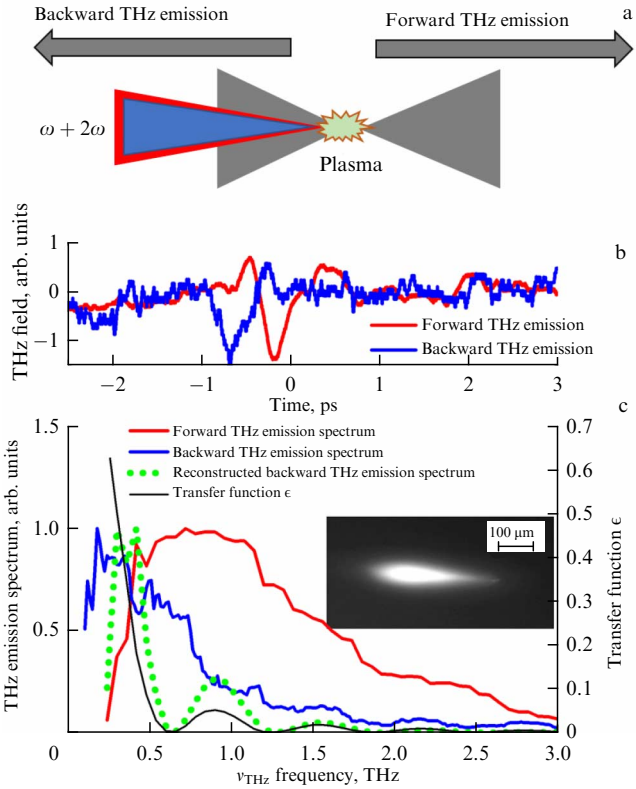


**Figure 3.** (a) Schematic of backward terahertz radiation production; (b) measured temporal shapes of backward (blue line) and forward (red line) THz emission pulses; (c) spectra obtained from the measured temporal shapes of forward (red line) and backward (blue line) THz emission pulses; calculated transfer function $\epsilon$ from backward to forward THz spectrum (black line); backward THz spectrum reconstructed from the direct spectrum according to simulation within the interference model. Inset corresponds to plasma luminescence recorded with a CMOS camera.

### 4.3 Terahertz emission from extended plasma channels

As noted in the foregoing, the optical-to-terahertz radiation conversion efficiency depends critically on the phase between harmonics [30]. In atmospheric air, a phase shift of $\pi$ between the fundamental (800 nm) and second (400 nm) harmonics of a titanium-sapphire laser occurs at a distance of about 25 mm. In the filamentation of laser radiation in gases, the length of plasma channels can be many times greater than this distance, which inevitably leads to a change in the conditions of phase matching along the channel. It was shown in Ref. [59] that this effect results in an off-axis peak in the angular THz distribution.

The general approach to the generation of terahertz radiation in extended channels is that the field at each point in space is the result of the interference of waves from a set of local sources (dipoles) in the plasma channel [59, 62, 78, 79]. The generation efficiency of such sources depends on the phase between harmonics and the local plasma density, and the phase of the terahertz field depends on the distance to the observation point and on the part of the distance traversed during propagation through the plasma. In Ref. [78], the possibility of controlling the carrier-envelope phase in a detected terahertz pulse was demonstrated by adjusting the distance from the frequency doubling crystal to the beginning of the plasma channel (the initial phase mismatch between the fundamental and second harmonics) and by changing the length of the plasma channel.

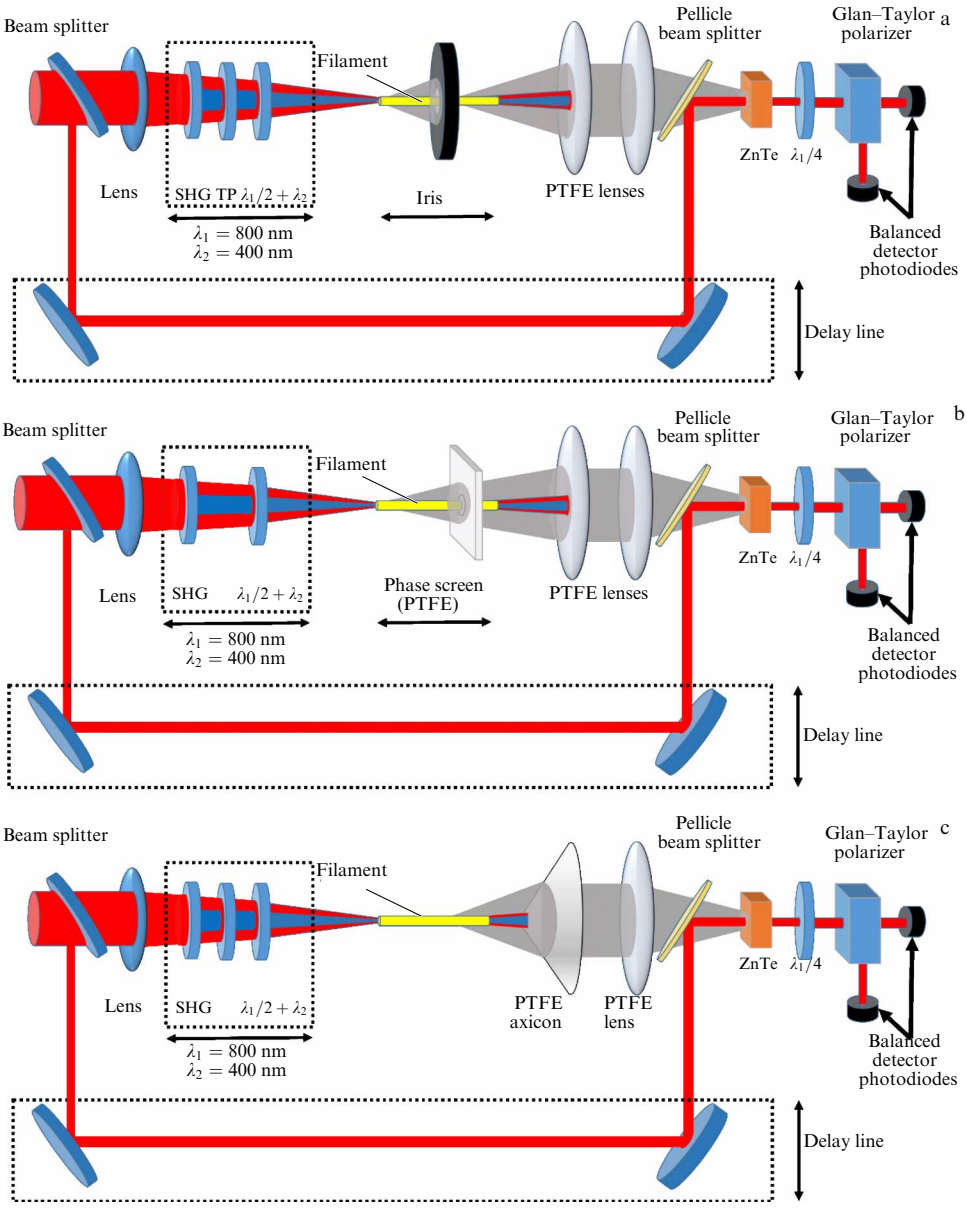


**Figure 4.** Schematics of experimental setups (a) for studying the generation of THz radiation in a long plasma channel; (b) for spectral modulation using phase screens; (c) for spectral filtering using an axicon.

Reference [79] demonstrated the possibility of frequency filtering of the spectrum of a terahertz pulse through the use of interference. Two approaches were proposed: the use of phase screens and the use of axicons to collect the terahertz radiation emerging from an extended plasma channel (see Fig. 4). In the former approach, screens are installed along the plasma channel in such a way as to provide constructive interference for the selected terahertz frequency due to a phase addition of $\pi$ rad at a given frequency. The second approach is based on the fact that the maximum intensity for individual terahertz frequencies is observed at different angles relative to the optical axis [59, 62, 64]. So, the axicon angle determines the terahertz frequency that will be collected most efficiently.

In a recent paper [80], an investigation was made of the influence of the initial phase mismatch between harmonics on the spectral characteristics of radiation from an extended filament. It was found that low-frequency radiation ($< 5$ THz) is significantly affected by the phase mismatch, while the high-frequency (5–20 THz) part of the signal experiences only slight modulation. So, the initial phase mismatch allows one to control the spectrum of the THz pulse.

## 5. Influence of the chirp of femtosecond laser pulses

In the generation of terahertz radiation in a plasma using two-color pulses, use is made mainly of laser systems operating by the principle of chirped pulse amplification [81]. In such systems it is possible to control the magnitude and sign of the chirp of the output radiation. The effect of pulse chirp on the generation of terahertz radiation in a laser plasma using two-color pump pulses has been noted in several papers [54, 82, 83]. It turns out that the maximum conversion efficiency is achieved with a small positive chirp of the original pulse, and

not with a spectrally limited pulse [54, 84]. A local minimum of emission efficiency is observed for a small negative chirp, and, in general, a negative-sign chirp is less productive. The explanation for this behavior is a better time overlap between pulses when using a slightly stretched pulse in the second harmonic generation in a nonlinear crystal, in which, among other things, a delay of the second harmonic pulse is observed due to dispersion. However, stretching the pulse to significant durations results in a lower laser intensity and worse nonlinear conversion to the second harmonic and, subsequently, to terahertz radiation. Furthermore, one should take into account the change in the relative phase between the harmonics of a two-color pulse, which, in order to achieve optimal conversion for the selected pulse duration, requires compensation either by moving the converter crystal or by using compensation optical elements (pairs of quartz wedges, calcite plates, or $\alpha$-BBO). Xu et al. [83] observed the dependence of the terahertz radiation spectrum on the chirp magnitude.

Another example of controlling the parameters of generated THz radiation by using the temporal-frequency characteristics of a laser pulse is Ref. [85], where the possibility of tunable narrow-band THz generation with a controllable carrier-envelope phase was demonstrated in the optical breakdown of air by spectrally modulated pulses.

## 6. Effect of pump radiation wavelengths

When considering the generation mechanism from the point of view of multi-wave mixing, the 1:2 component frequency ratio of the two-color pulse turns out to be optimal, since it requires cubic nonlinearity of the medium for optical rectification. The use of other frequency ratios requires higher-order nonlinearities. With the advent of the photocurrent model, interest in nonstandard frequency ratios has appeared: in accordance with this model, the total instantaneous intensity of laser radiation and its asymmetry in a two-color pulse are important for the generation efficiency. For instance, according to theoretical research [86], harmonic ratios of 2:3 and 3:4 can be as effective as the standard 1:2. Such nonstandard ratios were experimentally studied in Ref. [87], where ratios 1:4 and 2:3 were used. It was demonstrated that emission at such frequency ratios is observed, its behavior is more consistent with the photocurrent mechanism rather than multiwavelength interaction, and it is also possible to control the polarization of THz radiation.

Also noteworthy is Ref. [88], where the fundamental harmonic of a titanium-sapphire laser (800 nm) was mixed with the radiation from a parametric amplifier near the halved harmonic (1600 nm). Observed were a resonant behavior of the generation efficiency near the halved frequency and an enhancement of high-frequency components of the spectrum with frequency detuning. A similar enhancement of the high-frequency components was also noted when detuning from the second harmonic frequency in Ref. [89].

As a continuation of the approach involving different ratios between harmonics, work with three-color pumping has appeared, where three pump pulses with different wavelengths interact simultaneously [90]. It is noteworthy that in this case there is both an increase in the output power and a broadening of the spectrum of terahertz radiation [91–93]. This fact is explained by a violation of the periodicity of ionization events in time, which forms a temporal structure similar to an aperiodic diffraction grating for radiation in the THz range corresponding to the zero diffraction order.

The next issue is the optimization of pump laser wavelengths (with a standard ratio of 1:2) for efficiently generating terahertz radiation from plasma. Here, a number of theoretical papers demonstrate an increase in the generation efficiency with increasing fundamental harmonic wavelength; in particular, Ref. [40] reports an increase in the THz radiation power by an order of magnitude with the use of pulses at a wavelength of 2 μm compared to the most common case of 0.8 μm. Later, it was shown in [94] that the highest generation efficiency is achieved in the region of 3.2 μm in considering the wavelength range from 0.8 to 10.6 μm, while shifting to the long-wavelength region of the pump pulses results in a decrease in the divergence angle of terahertz radiation. Another paper [95] also reported an increase in the output power of THz radiation with a shift from the visible to the infrared region of 1.5–4 μm. In many ways, the highest optimum output power here was determined by the focusing conditions. For a three-color scheme ($\omega + 2\omega + 3\omega$), a shift of the fundamental frequency to 4 μm also causes an increase, as in the case of a two-color scheme [96]. Flender et al. [97] expanded the range of wavelengths under consideration from 2.15 μm to 15.15 μm, indicating that there are a number of local maxima in this region and that the global maximum is located in the vicinity of 12.3 μm.

Apart from traditional research using titanium-sapphire lasers (800 nm + 400 nm), the generation of THz radiation was demonstrated with the use of an ytterbium laser (main radiation wavelength: 1030 nm) [98], the combination 1600 nm + 800 nm (titanium-sapphire laser and parametric amplifier) [88], a thulium fiber laser (main wavelength: 1920 nm) [99], a Yb:KGW laser with a parametric converter (main wavelength: 3900 nm) [23], a titanium-sapphire laser with a parametric converter (main wavelength: 1200–2600 nm) [100], and a titanium-sapphire laser with a parametric converter (main wavelength: 1225–2020 nm) [101]. The parameters of these investigations are collected in Table 2.

**Table 2.** Generation of THz radiation in a two-color setup at different wavelengths of pump radiation.

| Central pump wavelength in a two-color generation setup (first and second harmonics), μm | Electric THz field strength, MV cm$^{-1}$ | Photon energy conversion efficiency | Central spectrum frequency, THz | Spectral emission band, THz |
|---|---|---|---|---|
| 0.8 [22] | 8 | $10^{-4}$ | $\sim 2$ | $> 100$ |
| 1.92 [99] | 10 | $3 \times 10^{-4}$ | $\sim 10$ | $\sim 35$ |
| 3.9 [23] | 100 | $2.4 \times 10^{-2}$ | $\sim 8$ | $\sim 15$ |
| 1.2–2.6 [100] | — | $10^{-4}$ | — | — |
| 0.8–2 [101] | 4.4 (1.85 μm) | $10^{-3}$ (1.85 μm) | 6 (1.85 μm) | 20 (1.85 μm) |

**Table 3.** Experiments on terahertz radiation generation in gas plasma under 800-nm + 400-nm pumping at varied pressure.

| Literature | Gases under study | Pressure, mbar | Laser pulse energy, mJ | Duration, fs | Focus length, cm | Maximum energy of THz pulse, μJ | Measured spectrum width, THz |
|---|---|---|---|---|---|---|---|
| [31] | $N_2$ | 3–20,000 | 0.18 | 150 | — | — | 2 |
| [103] | Air, $CO_2$ | 10–10,000 | 0.64 | 120 | 17 | 0.55 | 1.5 |
| [104] | Air, $N_2$, Ar, Kr, He | 10 – 580 | 2 – 18 | 50 | 15 | 5 | 75 |
| [105] | Air, Ar, Kr, Xe, Ne | 1 – 700 | 6 | 40 | 12.5 | 0.7 | 20 |
| [32] | Air, $N_2$, Ar, Kr, He, Ne | 10 – 580 | 2 – 18 | 50 | 12.5 – 40 | 5 | 75 |
| [106] | $N_2$, Cs, Rb | 0.025–0.67 | 0.06–0.6 | 50 | — | — | 8 |
| [107] | $N_2$, $H_2O$, $D_2O$ | 0–1000 | 1 | 100 | 10 | — | 8 |
| [110] | Air, $N_2$, Ar | 0.2–1500 | 1–80 | 30–500 | 25 | 1.5 | 6 |

It is quite difficult to unambiguously compare all the presented results, since they lead to different focusing conditions, durations, and pulse energies, but comparative studies within the same work clearly show an increase in the THz radiation generation efficiency when the fundamental harmonic wavelength is shifted to the mid-infrared range.

## 7. Influence of properties of the gaseous medium on the generation of terahertz radiation

Gas pressure significantly affects the parameters of the resulting laser plasma [102] and the nonlinear response of the medium. The first work to study the effect of gas pressure on the THz radiation generation efficiency in the case of two-color pumping was Ref. [31], where the nitrogen pressure was varied in a broad range from 3 mbar to 20 bar. The authors identified 3 domains: 3–100 mbar, an increase in generation efficiency, which they explained by complete ionization of the gas; 100 mbar–2 bar, a mode with a weak change in the THz radiation power with an optimum in the vicinity of 1 bar, which was attributed to an increase in the influence of defocusing in the plasma and saturation of the product of the plasma volume and its density; 2–20 bar, a decrease in the generation efficiency, which was attributed to an increase in electron scattering by molecules, which has a destructive effect on the macroscopic photocurrent. A decrease in the generation efficiency with increasing pressure in air and carbon dioxide was also noted in Ref. [103]. An optimum in the low-frequency domain of the spectrum ($< 2$ THz) was also noted near 1–2 bar.

The emergence of methods for measuring the spectral power of THz radiation pulses in the range above 3 THz has shown that the main power of THz radiation from laser plasma produced by two-color pulses lies precisely in the high-frequency region. As shown in Refs [32, 104, 105], the optimum optical-terahertz conversion is achieved at pressures below atmospheric. Furthermore, gases with low ionization potentials exhibit a poorer THz radiation generation efficiency. It is worth noting that the relative phase between harmonics changes as the laser radiation propagates along a plasma channel due to dispersion in the plasma, which results in modulation of the conversion efficiency [105]. In this case, the modulation amplitude increases with increasing laser pulse energy, but decays faster with increasing gas pressure.

The generation of THz radiation has also been studied in tenuous vapors of metals such as rubidium and cesium, where a significant increase in generation is observed due to the low ionization potential [106]. Generation in tenuous water vapor and in water clusters in a gas jet has also been demonstrated [107], which is of special interest in view of the strong absorption of water molecules in the THz range (see Table 3).

In addition, it has been noted that it is possible to control the THz radiation generation efficiency in an extended filament with a local change in plasma density by using a gas jet [108, 109].

## 8. Generation of terahertz radiation in multiple and super filamentation

The phenomenon of filamentation has been known to the scientific community since the 1960s in connection with the development of laser sources. The cause of filamentation was the self-focusing mechanism, in which a nonlinear change in the refractive index of a substance occurs under the influence of laser radiation. In this case, the general expression for the refractive index is defined as follows:

$$n = n_0 + n_2 I + n_4 I^2 + n_6 I^3 + n_8 I^4 + n_{10} I^5 + \dots , \qquad (7)$$

where $n_0$ is the linear refractive index, $n_2$, $n_4$, $n_6$, $n_8$, $n_{10}$ are nonlinear refractive indices, and $I$ is the radiation intensity.

When considering only the first two terms in the expression for the refractive index for the propagation of, for example, a Gaussian beam (which is close in its properties to real laser beams), the radiation intensity in the paraxial region is always higher than at the periphery, with the result that the laser beam forms a medium reminiscent in its properties of a lens design. In this way, laser radiation can be focused without any additional optical elements.

For a significant increase in intensity, subsequent terms in Eqn (4) also begin to make a significant contribution, which inevitably leads to a change in plasma parameters that ensure the attainment of equilibrium between focusing and defocusing required for the existence of a filament. The change in the refractive index (or refractive index anisotropy) of a medium exposed to high-intensity laser radiation can be determined in pump-probe experiments. The values of $n_4$, $n_6$, $n_8$, and $n_{10}$ for various gases were measured in Ref. [111] with close to co-directional propagation of pump and probe pulses. It should be noted that, in addition to the Kerr effect, the alignment of molecules under laser irradiation contributes to anisotropy, and, due to this effect, periodic restoration of such anisotropy is observed with a time interval of several picoseconds after the passage of high-power radiation [111–113]. With an orthogonal geometry of the propagation of pump and probe radiation pulses, refractive index anisotropy was visualized in ultrafast

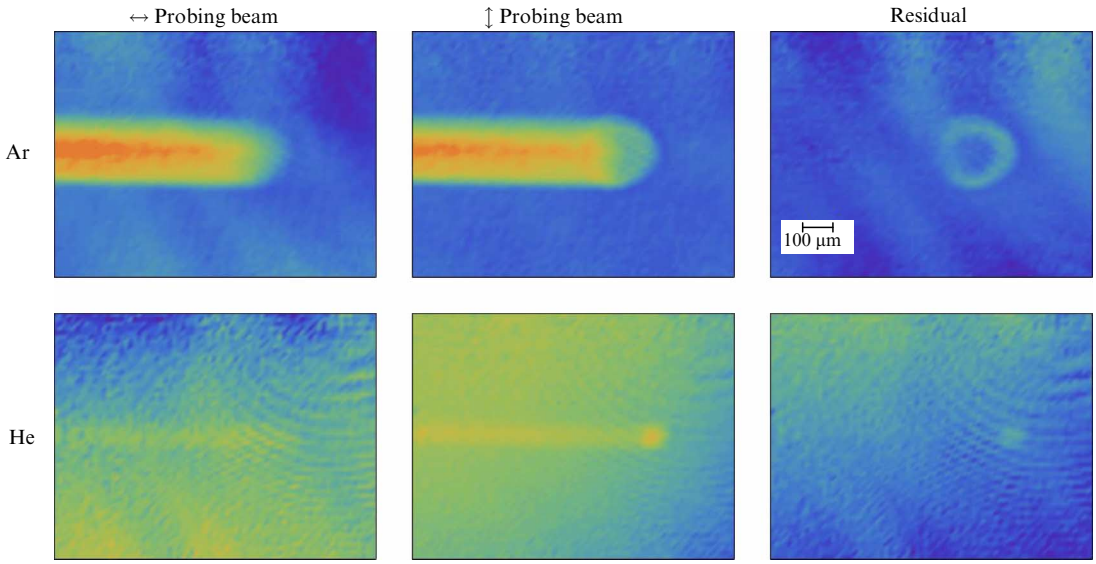


**Figure 5.** Images of phase additive at the instant of channel formation when polarization of transmission beam changes, testifying to anisotropy of the refractive index. (↔ — horizontally polarized probing pulse; ↕ — vertically polarized probing pulse for a vertically polarized ionizing pulse.)

photography experiments with crossed polarizers [112, 113] and in a scheme with interferometric recording of changes in the probe beam [114, 115]. The interferometric recording scheme, in addition to observing the anisotropy induced in the medium, also allows one to visualize the propagation of the ionization front in the medium and restore the distribution of the plasma electron density, and to observe, with increasing probing pulse delay, the dynamics of its recombination [102, 114, 116].

Figure 5 shows pictures of the observed anisotropy-induced phase shift in argon and helium [114, 115]. When the sign of the additive to the refractive index changes as the laser radiation intensity increases, the phase shift in the intense part of the pulse decreases (or even changes sign), resulting in the formation of a ring-shaped structure in the phase image (argon). Where the sign change does not occur (helium), the phase shift due to the anisotropy of the refractive index is a 'spot.'

Due to the finite size of laser beams, diffraction is inevitable, which competes with self-focusing. Therefore, generally speaking, there is a parameter that determines the threshold of this process — the critical self-focusing power, determined by the expression

$$P_{\rm cr} = \frac{3.77\lambda^2}{8\pi n_0 n_2} \,. \tag{8}$$

Here, $\lambda$ is the radiation wavelength. When the contributions from the self-focusing and diffraction cancel out, a stable regime called self-channeling can set in, in which the beam can propagate without changing its size over sufficiently long distances.

A situation is also possible in which the contribution of self-focusing exceeds diffraction effects, and then plasma production can occur due to field ionization: in this case, an additional contribution to the defocusing of laser radiation occurs. The additional term to the refractive index associated with the plasma production is defined by the expression

$$\Delta n \approx -\frac{\omega_p^2}{2\omega^2} \,. \tag{9}$$

When the contributions from plasma defocusing, diffraction, and self-focusing are equalized, laser radiation can also propagate over fairly large distances, by analogy with self-channeling, and extended threads are formed in this case — filaments. Inherent in pulses with a peak power tens of times higher than $P_{\rm cr}$ is a phenomenon in which they decay into many filaments. In this case, the decay itself occurs due to the spatial modulation instability of a high-intensity optical field in a medium with third-order nonlinearity. Due to chaotic disturbances in the intensity and phase of the optical field, which arise for a number of fundamental reasons (field distribution at the output of the laser system, fluctuations of the refractive index in the medium, scattering), the production of nonlinear foci occurs. This effect, in turn, inevitably leads to a redistribution of intensity in the cross section of the beam with the subsequent production of several filaments. This process is negative for the generation of THz pulses due to the violation of coherence and polarization of THz radiation due to the phase shift from individual plasma channels [1]. It was recently shown that, at radiation powers significantly exceeding $P_{\rm cr}$, a process is possible when several filaments begin to interact with each other, making up a single channel — a superfilament [117]. In this case, nonlinear processes build up, and the source is more stable than the case of multiple filamentation, which is of interest to research groups for the generation of secondary radiation.

Despite the attractiveness of this mode of interaction of high-power laser radiation with gaseous media, the superfilament is considered in most scientific papers not as a source of terahertz radiation but as a subject of research [118]. In a number of studies, the laser beam is pre-modulated using special amplitude or phase masks to enable a clearer demonstration of the fusion of single filaments to make up a superfilament [119, 120]. In this case, it is possible to produce a quasi-superfilament at relatively low laser radiation powers and also to determine the influence of the superfilament and individual filaments involved in its production on the generation of terahertz radiation from optical breakdown plasma in a gaseous medium. Interference of THz radiation from such filaments or superfilaments can lead to amplification of THz radiation in the paraxial direction. For example, Song et al. [121] experimentally demonstrated the possibility of enhancing the total THz radiation signal by forming two separate plasma

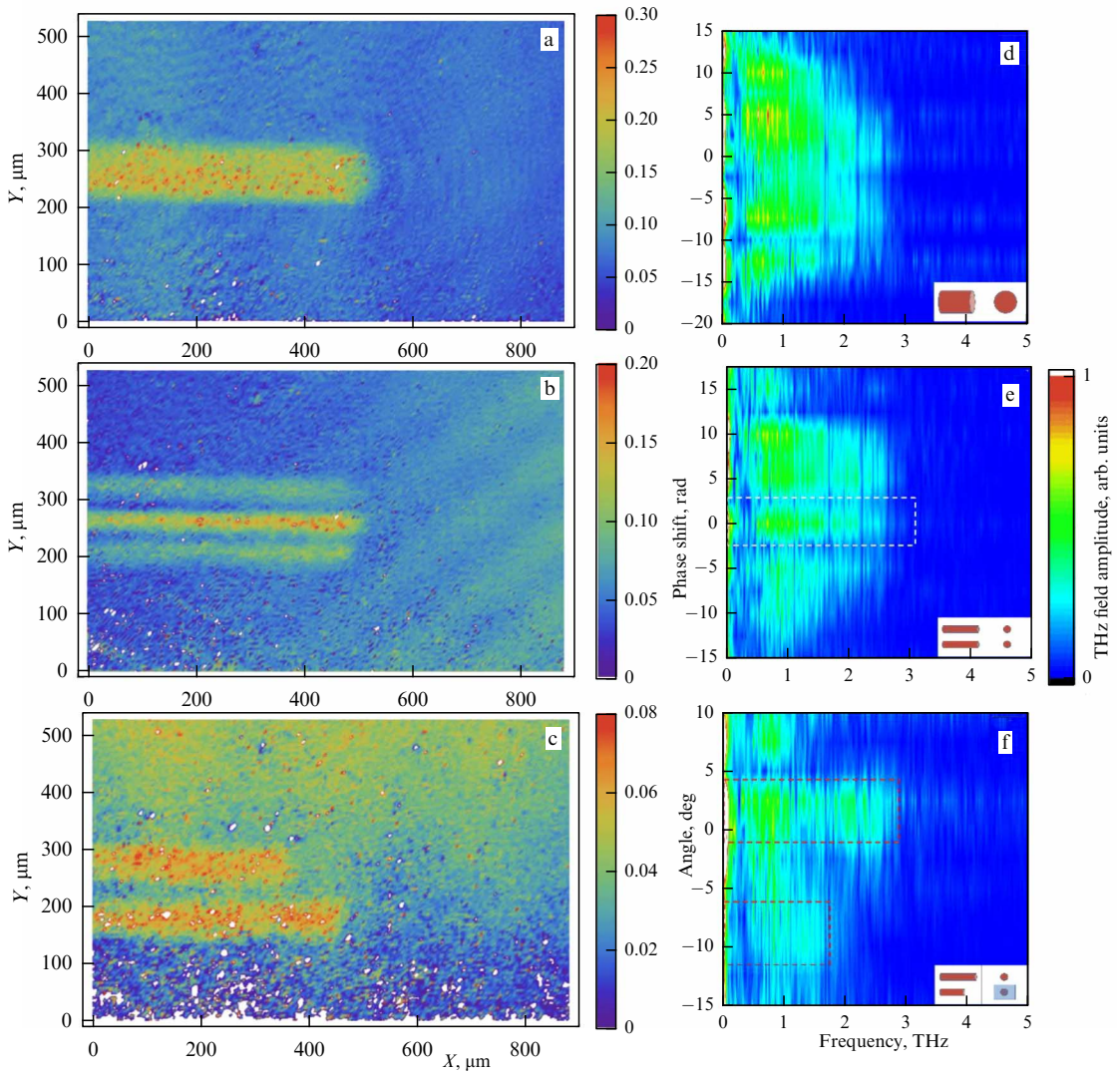


**Figure 6.** Phase shift in plasma channel recorded using interferometry. (a) Beam without a mask; (b) beam with a mask, simultaneously propagating pulses, and their interaction; (c) beam with a mask, delayed pulses, i.e., independent filaments; frequency-angular distributions of THz radiation amplitude: (d) free beam without a mask; (e) two regularized beams making up a superfilament-like structure; (f) two independent delayed filaments.

channels with an adjustable delay and a variable polarization state. However, in earlier modeling [69] and experiment [122], a conical power distribution of the generated terahertz radiation is produced in the presence of several noninteracting channels. Therefore, it is important to determine the optimized state for generating THz radiation and develop methods to control the spatial distribution of THz radiation for a two-color scheme. In Ref. [123], the proposed approach was implemented to generate THz radiation from a two-color laser plasma using amplitude modulation of pump laser radiation.

The plasma was formed by focusing laser radiation in the air, consisting of the fundamental and second harmonics with a linear co-directional polarization state. In this case, the delay between the fundamental and second harmonics was additionally compensated. The filaments were formed using an amplitude mask with holes; the independent production of channels was determined by introducing a quartz plate into one of the channels to bring about a delay several times longer than the duration of the initial pulses.

During the measurements, the pulse energy was recorded using a Golay detector, the temporal shapes of THz pulses propagating from the plasma at different angles to the axis were recorded using the electro-optical detection technique [42, 124], then the frequency-angular distributions were restored using the Fourier transform.

Pump–probe interferometry was used to characterize the plasma channel. The second probe beam was passed through optical delay line 2 and then through the central part of the plasma channel in the direction perpendicular to the optical axis. The probe beam refracted by the plasma was imaged by a telescope onto a Michelson interferometer. The phase shift in the plasma channel was probed immediately after ionization.

The experiments were carried out at a peak pulse power of about 20 GW. This figure is twice the critical power for self-focusing [125]. The following three versions of the plasma source were implemented: a single plasma channel formed by a free beam without a mask; interaction of filaments produced after two holes of the mask (for vertical and horizontal orientations of the holes), which corresponds to the recording of three channels in the distribution of phase shifts (the brightest central channel of the plasma corresponds to a superfilament-like structure); and independent production of two filaments due to the delay between the two parts of the beam (Fig. 6). In this case, the peak electron density for a

superfilament was $2.3 \times 10^{18}$ cm$^{-3}$, $1.4 \times 10^{18}$ cm$^{-3}$ for a single filament, and $7 \times 10^{17}$ cm$^{-3}$ for each of two delayed filaments.

A free beam (single filament) provides the highest THz radiation power. Three filaments produced by the interaction of two beams provide a lower level of THz radiation power. Two independent delayed filaments provide almost the same minimum power level as a single beam. The horizontal and vertical orientations of the mask holes do not lead to differences in the THz power in the paraxial region, so it can be assumed that the structure of the plasma channels does not change significantly. The resulting diagram of two delayed filaments is not the arithmetic sum of the THz radiation powers from each of the channels, indicating significant interference between these two sources.

The directional pattern has a maximum at $+5°$, without a symmetric maximum of THz radiation at $-5°$. This corresponds to an inclined intensity front caused by the delay of THz radiation from one of the plasma sources. When the mask is not used, the frequency-angular distribution is characteristic of the mode of moderate focusing of a two-color femtosecond pulse [42, 58, 59, 62, 64]. The THz radiation amplitude distribution is flat with an emerging conical structure with an opening angle of 5–10°. For a superfilament-like structure, a new THz component is produced, which propagates along the beam axis (at a zero angle). However, surrounding rings with a divergence angle of 5–10° also appear. So, the relation between the appearance of the axial component in the frequency-angular distribution of THz radiation and the interaction of filaments has been experimentally demonstrated. In fact, the interaction of filaments from different holes in the mask can be significantly suppressed by delaying the femtosecond radiation passing through one hole, relative to the radiation passing through the other hole, by an interval several times longer than the duration of the laser pulse. In this case, the filaments no longer interact. In the case of two lagging filaments, the conical spatial distribution prevails, and the axial component is negligible compared to the case of a superfilament-like structure.

In general, it can be noted that spatial modulation of pump radiation makes it possible to control the directional pattern of THz radiation and the structure of the plasma channel. However, it should be pointed out that the spatial modulation reduces the total energy of THz radiation, which apparently explains the small number of research papers in this field.

## 9. Conclusions

By and large, it can be noted that, over the past thirty years — since the publication of the first paper on the generation of terahertz radiation in laser plasma — extensive research has been carried out to optimize these types of sources, which significantly improved their potential applicability. Output levels of electric fields from tens to hundreds of MV cm$^{-1}$ allow the use of these sources for problems of nonlinear spectroscopy [126–128], force action [129], and remote diagnostics [130], as well as in different broadband terahertz spectrometers [131, 132] and physical facilities for studying the properties of materials using pump-probe techniques [133].

**Acknowledgments.** The authors express their gratitude to N A Panov, D E Shipilo, and I A Nikolaeva for fruitful discussions. The authors also thank the Ministry of Science and Higher Education of the Russian Federation for financial support under project no. 075-15-2020-790.

## References

1. Kandidov V P, Shlenov S A, Kosareva O G *Quantum Electron.* **39** 205 (2009); *Kvantovaya Elektron.* **39** 205 (2009)
2. Luo Q, Liu W, Chin S L *Appl. Phys. B* **76** 337 (2003)
3. Banerjee S et al. *Phys. Plasmas* **9** 2393 (2002)
4. Hamster H et al. *Phys. Rev. Lett.* **71** 2725 (1993)
5. Fattinger Ch, Grischkowsky D *Appl. Phys. Lett.* **54** 490 (1989)
6. Ferguson B, Zhang X-C *Nat. Mater.* **1** 26 (2002)
7. Siegel P H *IEEE Trans. Microwave Theory Tech.* **50** 910 (2002)
8. Golubev S V, Suvorov E V, Shalashov A G *JETP Lett.* **79** 361 (2004); *Pis'ma Zh. Eksp. Teor. Fiz.* **79** 443 (2004)
9. Lai C H et al. *Phys. Rev. Lett.* **77** 4764 (1996)
10. Löffler T, Jacob F, Roskos H G *Appl. Phys. Lett.* **77** 453 (2000)
11. Cook D J, Hochstrasser R M *Opt. Lett.* **25** 1210 (2000)
12. Wang T-J et al. *Appl. Phys. Lett.* **96** 211113 (2010)
13. Ushakov A et al. *Appl. Sci.* **11** 11888 (2021)
14. Balakin A V et al. *IEEE Trans. Terahertz Sci. Technol.* **7** (1) 70 (2017)
15. Ditmire T et al. *Phys. Rev. Lett.* **78** 3121 (1997)
16. Mori K et al. *Appl. Phys. Lett.* **111** 241107 (2017)
17. Solyankin P M et al. *Phys. Rev. Appl.* **14** 034033 (2020)
18. Jin Q et al. *Appl. Phys. Lett.* **111** 071103 (2017)
19. Ponomareva E A et al. *Opt. Express* **27** 32855 (2019)
20. Tcypkin A N et al. *Opt. Express* **27** 15485 (2019)
21. Dey I et al. *Nat. Commun.* **8** 1184 (2017)
22. Oh T I et al. *Appl. Phys. Lett.* **105** 041103 (2014)
23. Koulouklidis A D et al. *Nat. Commun.* **11** 292 (2020)
24. Jahangiri F et al. *Appl. Phys. Lett.* **99** 261503 (2011)
25. Shalaby M, Hauri C P *Nat. Commun.* **6** 5976 (2015)
26. Wu X et al. *Adv. Mater.* **35** 2208947 (2023)
27. Zhang X C, Shkurinov A, Zhang Y *Nat. Photon.* **11** 16 (2017)
28. Zhang L-L et al. *Phys. Rev. Appl.* **12** 014005 (2019)
29. Daranciang D et al. *Appl. Phys. Lett.* **99** 141117 (2011)
30. Kress M et al. *Opt. Lett.* **29** 1120 (2004)
31. Roskos H G et al. *Laser Photon. Rev.* **1** 349 (2007)
32. Kim K-Y et al. *IEEE J. Quantum Electron.* **48** 797 (2012)
33. Chizhov P A et al. *Quantum Electron.* **43** 347 (2013); *Kvantovaya Elektron.* **43** 347 (2013)
34. Kim K Y et al. *Opt. Express* **15** 4577 (2007)
35. Popov V S *Phys. Usp.* **47** 855 (2004); *Usp. Fiz. Nauk* **174** 921 (2004)
36. Keldysh L V *Sov. Phys. JETP* **20** 1307 (1965); *Zh. Eksp. Teor. Fiz.* **174** 921 (1964)
37. Ammosov M V, Delone N B, Krainov V P *Sov. Phys. JETP* **64** 1191 (1986); *Zh. Eksp. Teor. Fiz.* **91** 2008 (1986)
38. Borodin A V et al. *Opt. Lett.* **38** 1906 (2013)
39. Balakin A V et al. *J. Opt. Soc. Am. B* **27** 16 (2010)
40. Bergé L et al. *Phys. Rev. Lett.* **110** 073901 (2013)
41. Kolesik M, Moloney J V *Phys. Rev. E* **70** 036604 (2004)
42. Ushakov A A et al. *Opt. Express* **26** 18202 (2018)
43. Kosareva O et al. *Opt. Lett.* **35** 2904 (2010)
44. Xie X, Dai J, Zhang X-C *Phys. Rev. Lett.* **96** 075005 (2006)
45. Houard A et al. *Opt. Lett.* **33** 1195 (2008)
46. Dai J, Karpowicz N, Zhang X-C *Phys. Rev. Lett.* **103** 023001 (2009)
47. Ushakov A A et al. *Bull. Lebedev Phys. Inst.* **41** 200 (2014); *Kratk. Soobshch. Fiz. Fiz. Inst. Ross. Akad. Nauk* **41** (7) 31 (2014)
48. Volkov R V et al. *Laser Phys.* **25** 065403 (2015)
49. Chizhov P A et al. *Phys. Wave Phenom.* **22** 236 (2014); *Trudy Inst. Obshch. Fiz. Ross. Akad. Nauk* **70** 78 (2014)
50. Manceau J-M, Massaouti M, Tzortzakis S *Opt. Express* **18** 18894 (2010)
51. Kosareva O et al. *Opt. Lett.* **43** 90 (2018)
52. Tu Y-Y et al. *J. Opt. Soc. Am. B* **39** A83 (2022)
53. Wang L et al. *J. Opt. Soc. Am. B* **39** A68 (2022)
54. Mou S et al. *Photon. Res.* **11** 978 (2023)
55. Zhang Y et al. *Opt. Lett.* **47** 3816 (2022)
56. Zhong H, Karpowicz N, Zhang X-C *Appl. Phys. Lett.* **88** 261103 (2006)
57. D'Amico C et al. *Phys. Rev. Lett.* **98** 235002 (2007)
58. Borodin A V et al. *J. Opt. Soc. Am. B* **29** 1911 (2012)

59. You Y S, Oh T I, Kim K Y *Phys. Rev. Lett.* **109** 183902 (2012)
60. Oh T I et al. *New J. Phys.* **15** 075002 (2013)
61. Blank V, Thomson M D, Roskos H G *New J. Phys.* **15** 075023 (2013)
62. Gorodetsky A et al. *Phys. Rev. A* **89** 033838 (2014)
63. Buccheri F, Zhang X-C *Optica* **2** 366 (2015)
64. Andreeva V A et al. *Phys. Rev. Lett.* **116** 063902 (2016)
65. Shkurinov A P et al. *Phys. Rev. E* **95** 043209 (2017)
66. Yuan S et al. *J. Phys. B* **48** 094018 (2015)
67. Yuan S et al. *Opt. Express* **23** 5582 (2015)
68. Panov N A et al. *JETP Lett.* **93** 638 (2011); *Pis'ma Zh. Eksp. Teor. Fiz.* **93** 715 (2011)
69. Panov N et al. *Laser Phys. Lett.* **11** 125401 (2014)
70. Rasmussen M et al. *Opt. Express* **31** 9287 (2023)
71. Köhler C et al. *Opt. Lett.* **36** 3166 (2011)
72. Stremoukhov S Yu, Andreev A V *Laser Phys. Lett.* **12** 015402 (2015)
73. Ushakov A A et al. *JETP Lett.* **106** 706 (2017); *Pis'ma Zh. Eksp. Teor. Fiz.* **106** 675 (2017)
74. Ushakov A A et al. *Appl. Phys. Lett.* **114** 081102 (2019)
75. Rice A et al. *Appl. Phys. Lett.* **64** 1324 (1994)
76. Shipilo D E et al. *Photonics* **9** (1) 17 (2022)
77. Chen Y et al. *Sensors* **23** 4630 (2023)
78. Zhang Z et al. *Phys. Rev. Lett.* **117** 243901 (2016)
79. Chizhov P A et al. *Laser Phys. Lett.* **16** 075301 (2019)
80. Zhang Z et al. *Appl. Phys. Lett.* **123** 031108 (2023)
81. Strickland D, Mourou G *Opt. Commun.* **56** 219 (1985)
82. Yiwen E et al. *Appl. Phys. Lett.* **113** 181103 (2018)
83. Xu X et al. *Chinese Phys. Lett.* **40** 045201 (2023)
84. Zhang Z et al. *Appl. Phys. Lett.* **113** 241103 (2018)
85. Zhou X et al. *Opt. Lett.* **48** 2881 (2023)
86. Kostin V A et al. *Phys. Rev. Lett.* **117** 035003 (2016)
87. Zhang L-L et al. *Phys. Rev. Lett.* **119** 235001 (2017)
88. Vvedenskii N V et al. *Phys. Rev. Lett.* **112** 055004 (2014)
89. Fan Z, Lu C, Liu Y *Opt. Commun.* **505** 127532 (2022)
90. Ma D et al. *Opt. Commun.* **481** 126533 (2021)
91. Bagley J D et al. *J. Phys. B* **51** 144004 (2018)
92. Vaičaitis V et al. *J. Appl. Phys.* **125** 173103 (2019)
93. Petersen P B, Tokmakoff A *Opt. Lett.* **35** 1962 (2010)
94. Fedorov V Yu, Tzortzakis S *Opt. Express* **26** 31150 (2018)
95. Nikolaeva I A et al. *Photonics* **9** 974 (2022)
96. Wang S et al. *J. Opt. Soc. Am. B* **37** 3325 (2020)
97. Flender R, Borzsonyi A, Chikan V *J. Opt. Soc. Am. B* **37** 1838 (2020)
98. Piccoli R et al. *Opt. Express* **27** 32659 (2019)
99. Buldt J et al. *Opt. Lett.* **48** 3403 (2023)
100. Nguyen A et al. *Opt. Lett.* **44** 1488 (2019)
101. Clerici M et al. *Phys. Rev. Lett.* **110** 253901 (2013)
102. Chizhov P A et al. *Quantum Electron.* **46** 332 (2016); *Kvantovaya Elektron.* **46** 332 (2016)
103. Solyankin P M et al. *New J. Phys.* **22** 013039 (2020)
104. Kim K Y et al. *Nat. Photon.* **2** 605 (2008)
105. Rodriguez G, Dakovski G L *Opt. Express* **18** 15130 (2010)
106. Sun X, Zhang X-C *Appl. Phys. Lett.* **104** 191106 (2014)
107. Johnson K et al. *Phys. Lett. A* **372** 6037 (2008)
108. Chizhov P A et al. *Bull. Lebedev Phys. Inst.* **46** 333 (2019); *Kratk. Soobshch. Fiz. Fiz. Inst. Ross. Akad. Nauk* **46** (11) 3 (2019)
109. Xiao H et al. *Phys. Rev. A* **104** 013517 (2021)
110. Nazarov M M et al. *J. Infrared Millimeter Terahertz Waves* **41** 1069 (2020)
111. Loriot V et al. *Opt. Express* **17** 13429 (2009)
112. Fujimoto M et al. *Opt. Lett.* **24** 850 (1999)
113. Fujimoto M, Aoshima S, Tsuchiya Y *Meas. Sci. Technol.* **13** 1698 (2002)
114. Chizhov P, Bukin V, Garnov S *Phys. Procedia* **71** 222 (2015)
115. Chizhov P A, Bukin V V, Garnov S V *J. Phys. Conf. Ser.* **666** 012018 (2016)
116. Bodrov S et al. *Opt. Express* **19** 6829 (2011)
117. Point G et al. *Phys. Rev. Lett.* **112** 223902 (2014)
118. Samsonova Z et al. *Phys. Rev. A* **97** 063841 (2018)
119. Pushkarev D et al. *New J. Phys.* **21** 033027 (2019)
120. Pushkarev D et al. *Laser Phys. Lett.* **15** 045402 (2018)
121. Song Q et al. *Opt. Express* **29** 22659 (2021)
122. Jahangiri F et al. *Appl. Phys. Lett.* **102** 191106 (2013)
123. Ushakov A et al. *Photonics* **8** (1) 4 (2021)
124. Chizhov P A et al. *Quantum Electron.* **45** 434 (2015); *Kvantovaya Elektron.* **45** 434 (2015)
125. Liu W, Chin S L *Opt. Express* **13** 5750 (2005)
126. Chai X et al. *Opt. Lett.* **43** 5463 (2018)
127. Vicario C, Shalaby M, Hauri C P *Phys. Rev. Lett.* **118** 083901 (2017)
128. Hoffmann M C et al. *Appl. Phys. Lett.* **95** 231105 (2009)
129. Agranat M B et al. *Phys. Rev. Lett.* **120** 085704 (2018)
130. Talbi A et al. *Europhys. Lett.* **143** 10001 (2023)
131. Bergé L et al. *Europhys. Lett.* **126** 24001 (2019)
132. Zhou B et al. *Sensors* **23** 3669 (2023)
133. Yada H et al. *Appl. Phys. Lett.* **105** 143302 (2014)